OCEAN THERMAL STRUCTURE RESPONSE TO A MOVING HURRICANE MODEL

Robert Norris Trapnell

NAVAL POSTGRADUATE SCHOOL
Monterey, California

THESIS

OCEAN THERMAL STRUCTURE RESPONSE
TO A MOVING HURRICANE MODEL

by

Robert Norris Trapnell, Jr.

September 1974

Thesis Advisors: R. L. Elsberry
D. F. Leipper

UNCLASSIFIED

SECURITY CLASSIFICATION OF THIS PAGE (When Data Entered)

REPORT DOCUMENTATION PAGE		READ INSTRUCTIONS BEFORE COMPLETING FORM
1. REPORT NUMBER	2. GOVT ACCESSION NO.	3. RECIPIENT'S CATALOG NUMBER
4. TITLE (and Subtitle) Ocean Thermal Structure Response To A Moving Hurricane Model		5. TYPE OF REPORT & PERIOD COVERED Master's Thesis; September 1974 6. PERFORMING ORG. REPORT NUMBER
7. AUTHOR(s) Robert Norris Trapnell, Jr.		8. CONTRACT OR GRANT NUMBER(s)
9. PERFORMING ORGANIZATION NAME AND ADDRESS Naval Postgraduate School Monterey, California 93940		10. PROGRAM ELEMENT, PROJECT, TASK AREA & WORK UNIT NUMBERS
11. CONTROLLING OFFICE NAME AND ADDRESS Naval Postgraduate School Monterey, California 93940		12. REPORT DATE September 1974 13. NUMBER OF PAGES 53
14. MONITORING AGENCY NAME & ADDRESS (if different from Controlling Office) Naval Postgraduate School Monterey, California 93940		15. SECURITY CLASS. (of this report) Unclassified 15a. DECLASSIFICATION/DOWNGRADING SCHEDULE

16. DISTRIBUTION STATEMENT (of this Report)

Approved for public release; distribution unlimited.

17. DISTRIBUTION STATEMENT (of the abstract entered in Block 20, if different from Report)

18. SUPPLEMENTARY NOTES

19. KEY WORDS (Continue on reverse side if necessary and identify by block number)

Air-Sea Interaction
Advection
Hurricane Model
Ocean Model
Convective Mixing
Wind Mixing

20. ABSTRACT (Continue on reverse side if necessary and identify by block number)

The time-dependent mixed-layer depth and temperature response of a two-layer ocean model to a moving hurricane model was investigated. The hurricane model was that of Elsberry, Pearson, and Corgnati (1974). The maximum hurricane wind was bounded at 50 m/sec in order to isolate ocean reactions from hurricane variance. The ocean model was based on that of Fraim (1973) which was derived from the earlier mixed-layer models of Kraus and Turner (1967)

DD FORM 1 JAN 73 1473 EDITION OF 1 NOV 65 IS OBSOLETE
S/N 0102-014-6601 | 1
(Page 1)

UNCLASSIFIED
SECURITY CLASSIFICATION OF THIS PAGE (When Data Entered)

Block #20 Continued.

and Denman (1973). The ocean model was an idealized, quasi-three-dimensional model designed to examine the effects along the path of movement due to the passage of a moving hurricane. Results indicated that slower-moving storms engendered the greatest change in mixed-layer depth and temperature. Away from the center a combination of entrainment mixing and convection was responsible for the majority of the depth and temperature changes. Near the eye, in the upwelling zone, a combination of entrainment mixing, convection, and advection caused temperature change while advection alone dominated layer depth change.

Ocean Thermal Structure Response To A Moving Hurricane Model

by

Robert Norris Trapnell, Jr.
Captain, United States Air Force
B.S., University of Texas, 1969

Submitted in partial fulfillment of the
requirements for the degree of

MASTER OF SCIENCE IN OCEANOGRAPHY

from the

NAVAL POSTGRADUATE SCHOOL
September 1974

ABSTRACT

The time-dependent mixed-layer depth and temperature response of a two-layer ocean model to a moving hurricane model was investigated. The hurricane model was that of Elsberry, Pearson, and Corgnati (1974). The maximum hurricane wind was bounded at 50 m/sec in order to isolate ocean reactions from hurricane variance. The ocean model was based on that of Fraim (1973) which was derived from the earlier mixed-layer models of Kraus and Turner (1967) and Denman (1973). The ocean model was an idealized, quasi-three-dimensional model designed to examine the effects along the path of movement due to the passage of a moving hurricane. Results indicated that slower-moving storms engendered the greatest change in mixed-layer depth and temperature. Away from the center a combination of entrainment mixing and convection was responsible for the majority of the depth and temperature changes. Near the eye, in the upwelling zone, a combination of entrainment mixing, convection, and advection caused temperature change while advection alone dominated layer depth change.

TABLE OF CONTENTS

LIST OF TABLES

LIST OF FIGURES

Figure

ACKNOWLEDGEMENTS

The author wishes to express his thanks to Dr. R. L. Elsberry for his time, patience, and guidance; Dr. D. F. Leipper for his time and comments; and Dr. R. L. Haney for his comments.

The author also wishes to thank the personnel of the William R. Church Computer Center, especially: Mr. W. D. Ehrman, consultant, for his time and help in writing the model, and Mr. E. Donnellan, swing-shift supervisor, for his expedition of many jobs and unfailing humor.

I. INTRODUCTION

There exists a large body of evidence which demonstrates that there is a complex interaction between a hurricane and the ocean. For example it appears that sea-surface temperatures in excess of 26 C are required to produce hurricane-force winds. Through these winds, the hurricane imparts stress to the ocean, which acts as a sink for the hurricane's momentum. Interactions have been modeled in several ways. It is apparent that for an ocean-interacting hurricane model to be valid, the heat-momentum energy-exchange balance must be satisfied.

Elsberry, Pearson, and Corgnati (1974) developed an axisymmetric, ocean-interacting hurricane model which met the energy balance conditions. A description of the air-sea interaction within the boundary-layer of a hurricane was the output of and the primary purpose for the design of the model. For this purpose, a stationary, mature hurricane over a constant, isothermal ocean was assumed. The capability for interaction with a time-dependent ocean model was included in the design.

One of the uses envisioned for the model described above was to investigate the cause of low sea-surface temperatures found in the wake of a hurricane. Based on limited observations following tropical cyclones, wind mixing, convective mixing, and upwelling appear to be the main cooling mechanisms. Jordan (1964) concluded that mixing was dominant.

Fischer (1958) mentioned upwelling as being important. Leipper (1967) found upwelling to be dominant near the eye with a transition to convective and/or mechanical mixing dominance at greater radii. The classical model by O'Brien and Reid (1967) and O'Brien (1967) simulated a stationary hurricane with constant forcing over a one-layer ocean. Results of the model emphasized the importance of upwelling and downwelling. Gilbert (1974) modeled a stationary, time-dependent hurricane over a multi-layer ocean. Results of the Gilbert model indicate transitory inertial oscillations exert as much influence as the steady-state wind.

Fraim (1973) developed a time-dependent, two-layer model for the ocean only based on the earlier mixed-layer models of Kraus and Turner (1967) and Denman (1973). The model was driven by the time-dependent, axi-symmetric, stationary hurricane model of Elsberry, *et. al.* (1974). The axi-symmetric assumption permitted representation of the hurricane and the ocean by a radial cross-section assumed to be the integrated average of all radial cross-sections. Fraim (1973) concluded that a combination of entrainment mixing and upwelling was the major factor in changing the mixed-layer temperature and depth.

One of several logical extensions of the model was to use it to examine the effects on the ocean induced by a moving hurricane. One purpose for moving the storm was to consider Geisler's (1970) internal wake theory. The theory involves a comparison of the hurricane translational speed

(U) with the baroclinic wave speed (C). For a slow moving storm ($U/C < \sqrt{2}$), Geisler postulated upwelling and resultant surface cooling. For a fast moving storm ($U/C > 2$), Geisler postulated an internal wave wake at the interface between the mixed layer and thermocline. It should be emphasized that while Geisler's model and a similar model by O'Brien (1968) were primarily hydrodynamic, the model under study here was thermodynamic in nature.

The present model was originally designed to be fully a three-dimensional model. However, due to computer time and storage constraints, the model was made to represent a vertical cross-section of the ocean along which the storm was moved. The storm was translated at several typical speeds (including $U = 0$) in order to determine the effects of movement on changes in the mixed-layer depth and temperature.

II. DESCRIPTION OF THE MODEL

A. THE HURRICANE MODEL

The hurricane model was a two-layer, time-dependent model by Elsberry, Pearson, and Corgnati (1974). By assuming the hurricane to be mature, an assumption of axi-symmetry could be made. A surface inflow layer and an upper outflow layer constituted the model. The tangential wind (V_θ) profile at the top of the inflow layer was taken to be

$$V_\theta r^{\frac{1}{2}} = \text{constant} \qquad (1)$$

at radii outside the radius of maximum wind r_i. Inside r_i the winds were assumed to obey

$$V_\theta r^{-1} = \text{constant}. \qquad (2)$$

Equations (1) and (2) were empirically derived from observations by Riehl (1963) and supported by observations by Gray and Shea (1973). The maximum extent of the storm was defined to be the radius (r_o) at which flow in the outflow layer turned from cyclonic to anti-cyclonic, i.e. $V_\theta = 0$. The radius of maximum wind was assumed to coincide with the eyewall radius, which was taken to be the radius at which the average of five adjacent values of equivalent potential temperature (θ_e) was a maximum. Since the eye-wall has been observed to be a region of massive latent heat flux due to evaporation, the maximum θ_e was strongly tied to the sea-surface temperature of the underlying water. An expression

for the maximum wind speed was determined by assuming a gradient balance between the wind field and the pressure field

$$\frac{1}{\rho}\frac{\partial P}{\partial r} = \frac{V_\theta^2}{r} + fV_\theta \tag{3}$$

(where f is the coriolis parameter) and using the relation

$$V_\theta^2 = \frac{V_{\theta_i}^2 r_i}{r} . \tag{4}$$

Integrating equation (3) from r_o to r_i gives

$$V_{\theta_i} = \frac{0.5r_o}{r_o - r_i}\left[-2f\sqrt{r_i r_o} - r_i \right. \tag{5}$$

$$\left. + \sqrt{4f^2(\sqrt{r_i r_o} - r_i)^2 + 10^6 \frac{r_o - r_i}{\rho r_o}(\theta_{e_i} - \theta_{e_o})}\right] .$$

From r_o to $2r_o$ the wind profile in (1) was modified to decrease exponentially to 5 meters/second as a transition zone to realistic boundary conditions in order to allow downwelling.

From observations by Riehl (1963), the surface pressure at the eyewall was defined by the relation

$$\delta p = 2.56\delta\theta_e \tag{6}$$

where the δ symbols indicate a deviation from p = 1005 millibars and θ_e=350 K. The radial pressure field was computed by integrating the gradient wind over the radius, using the wind speed from (1) and (2).

The atmospheric boundary-layer model consisted of a surface layer and a spiral layer above. Specification of the surface layer was by Monin-Obukhov similarity theory. Within

the surface layer, the surface roughness was a function of the stress at the surface. The spiral layer, a transition layer from radial to tangential flow, was specified by a modification of Ekman-layer theory. An iterative solution was used to match the two layers. Further details of the iterative solution can be found in Cardone (1969).

A simple model for the hurricane was required to keep computer time and storage requirements to a minimum. Comparatively simple specification of the boundary layer and lack of specification of upper layers enabled compliance with those requirements. The axi-symmetric assumption allowed representation of the storm by a radial cross-section. Again, computational considerations required such an assumption. A friction velocity for the computation of water velocities and kinetic energy gain, and the heat flux were provided to the ocean model by the hurricane model. A new radial distribution of mixed-layer temperature was predicted by the ocean model, and then provided to the hurricane model. This type of interaction can lead to storm intensification. However, for the purposes of this study, the hurricane maximum wind was bounded at 50 m/sec. This enabled isolation of changes in the ocean.

B. THE OCEAN MODEL

1. Description of the Model

The ocean model was a modification of that by Fraim (1973), which was based on earlier mixed-layer models by Kraus and Turner (1967) and Denman (1972). The ocean was

assumed to have an initial mixed-layer depth of 30 m with a mixed-layer temperature of 30 C. The below-layer gradient was initially 0.1 C/meter to the top of an undisturbed layer defined by T = 20 C at Z = 130 meters. These values are typical of those found in the Gulf of Mexico and the Caribbean Sea in June, July, and August. The model was idealistic in that truly isothermal mixed layers and linear below-layer gradients are seldom found. Also, it would not be expected that the same thermal structure would exist over the whole ocean, or even any sizeable fraction of it.

There were several important modifications of the Fraim (1973) model. The Fraim model examined a radial cross-section of the ocean beneath a stationary hurricane. Equations for the ocean model were written in R-θ co-ordinates. The present model examined a vertical cross-section of the ocean along which the diametrical cross-section of the hurricane was allowed to move. The diametrical cross-section consisted of the radial cross-section used by Fraim and the mirror image of that radial cross-section. This was made possible by the assumption of axi-symmetry in the hurricane model. The ocean equations were written in cartesian co-ordinates on a 200 X 3 grid (see Figure 1) with a 6 kilometer grid whereas Fraim used a 100 X 1 grid with a 3 kilometer grid spacing. The time increment was 8 minutes compared to the 10 minute increment used by Fraim. A time increment of 8 minutes was used because it gave finer control over available translational speeds. The movement of

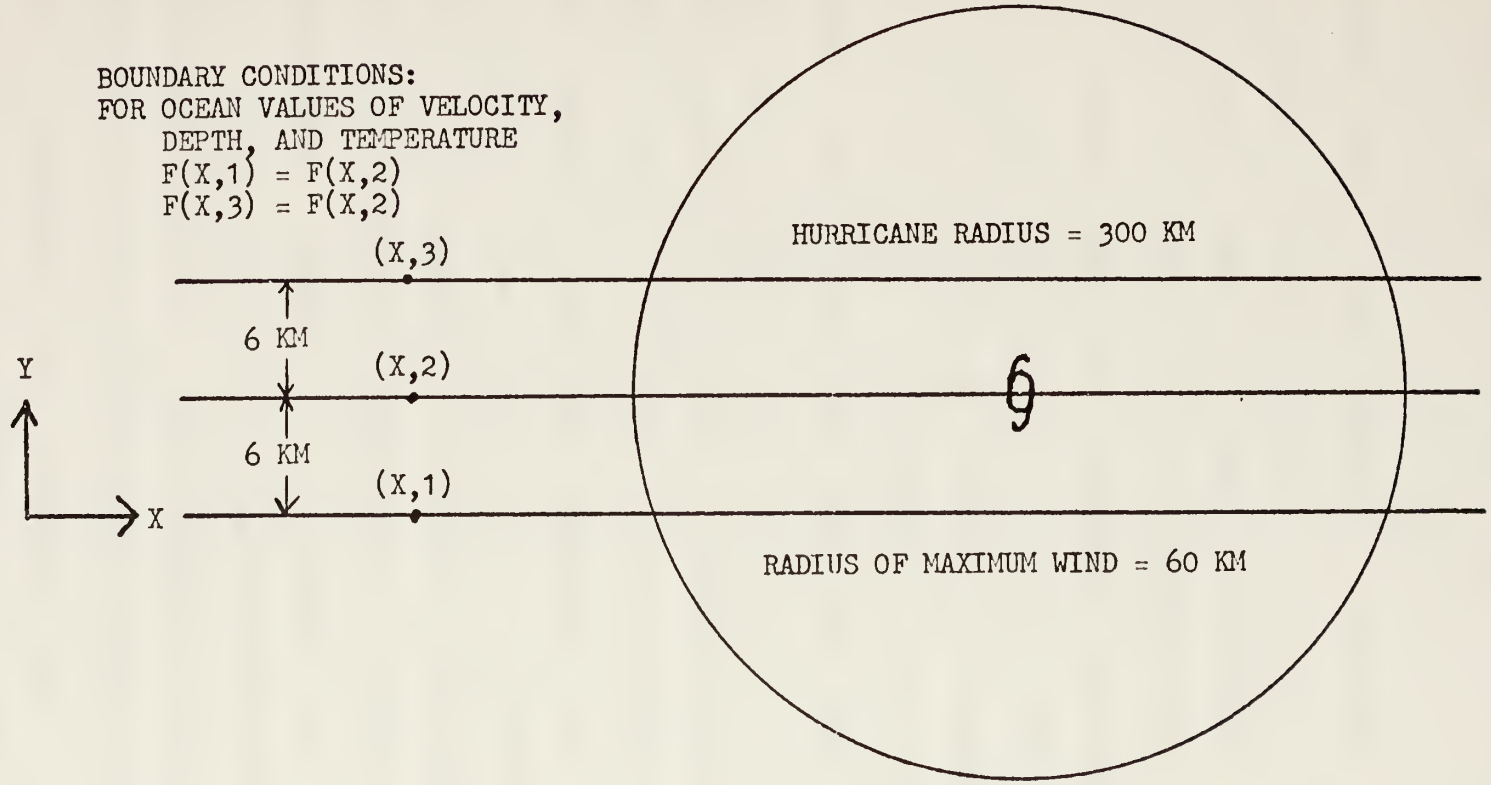

Figure 1. Schematic of Hurricane Moving Along 200 X 3 Grid in the Open Ocean.

the storm was achieved by moving the center of the storm to successive grid-points at time increments required to approximate the desired speed. Another modification was the addition of a horizontal return flow within the thermocline layer extending down to a specified layer of no motion. This closed the ocean system except for the radial advection, and thus improved the heat balance calculation for the stationary storm. Lastly, there was added to the model a convective adjustment for local convective instabilities.

Several important assumptions were made about the manner in which the ocean and hurricane would interact. First, since the storm was assumed to be mature at initiation, the wind stress was imparted to the ocean exponentially so that after 9 hours the ocean felt 95% of the stress. Second, some assumption had to be made as to what fraction of the stress would be used in inducing turbulence for entrainment mixing. The balance of the stress would be used in the creation of horizontal currents. With no pertinent data available it was decided to let entrainment dominate initially. An exponential transition dependent on the mixed-layer depth shifted the dominance to currents as the mixed layer deepened. Third, it was assumed that ocean currents began in Ekman balance and adjusted immediately to changes in the stress pattern. This assumption eliminates inertial waves which must be resolved using smaller time steps. Fourth, in examining only a vertical cross-section it was assumed that there was no variation in temperature or ocean

velocity across the path of the hurricane. This simplification was made because the net Ekman current should be normal to wind flowing inward at a specified angle, rather than being directed radially. Because of this, there was a resultant lack of symmetry across the path. This lack of symmetry introduced instabilities into the model. Fifth, it was assumed that the storm was wind dominated, implying that downward heat flux due to solar radiation was negligible.

The ocean model was forced by kinetic energy input due to wind stress, upward sensible heat fluxes, and upward latent heat flux due to evaporation. Horizontal currents due to wind stress were computed. Resultant upwelling and downwelling due to divergent and convergent current regimes were then determined. A new mixed-layer depth was calculated through kinetic energy, heat flux, and advection considerations. Based on the new mixed-layer depth, a new mixed-layer temperature was calculated. The below-layer gradient and temperature at the top of the thermocline were then determined. In this model the mixed-layer temperature and the temperature at the top of the thermocline can be different. If the temperature at the top of the thermocline was greater than the mixed-layer temperature a convective overturning process was initiated in order to stabilize the thermal structure. Following these calculations a radially averaged mixed-layer temperature was passed to the radial cross-section of the hurricane.

2. Derivation of the Model Equations

Following Denman (1973), the first law of thermodynamics can be written

$$\frac{dT}{dt} = \frac{Q_T}{\rho_w C_p} = \frac{\gamma R_* e^{-\gamma z}}{\rho_w C_p} \tag{7}$$

where $Q_T = R_* e^{-\gamma z}$, the heat source term,

ρ_w = ocean water density,

γ = average extinction coefficient,

C_p = specific heat at constant pressure,

R_* = solar radiation incident on the sea-surface, and

z = depth in the ocean, positive downward.

Expanding the total derivative in (7) yields

$$\frac{Q_T}{\rho_w C_p} = \frac{\partial T}{\partial t} + u\frac{\partial T}{\partial x} + v\frac{\partial T}{\partial y} + w\frac{\partial T}{\partial z} \tag{8}$$

where $w = \frac{dz}{dt}$ is positive for downward motion.
Time-averaging the turbulent form of (8) gives

$$\frac{Q_T}{\rho_w C_p} = \frac{\partial \overline{T}}{\partial t} + \frac{\partial \overline{uT}}{\partial x} + \frac{\partial \overline{vT}}{\partial y} + \frac{\partial \overline{wT}}{\partial z} + \frac{\partial \overline{w'T'}}{\partial z} = \frac{d\overline{T}}{dt} + \frac{\partial \overline{w'T'}}{\partial z} \tag{9}$$

or

$$\frac{d\overline{T}}{dt} = \frac{Q_T}{\rho_w C_p} - \frac{\partial \overline{w'T'}}{\partial z} \tag{10}$$

where the terms $\overline{u'T'}$ and $\overline{v'T'}$ were neglected because it was assumed that there was no systematic correlation between u' and v' and T'.

Turning now to an examination of the boundary conditions, firstly at the ocean surface, $z = 0$, a heat loss at

the sea surface will induce convective overturning which cools the mixed layer. Therefore, the downward turbulent heat flux $(\overline{w'T'})_o$ must equal the non-radiative heat loss, i.e.

$$(\overline{w'T'})_o = - \frac{Q_A}{\rho_w C_p} \tag{11}$$

where $Q_A = Q_E + Q_S$,

and Q_E = upward latent heat flux due to evaporation,

and Q_S = upward sensible heat flux.

At the base of the mixed layer downward turbulent heat flux is caused by wind-induced mixing and convective overturning. The turbulent heat flux must equal the heat transfer due to entrainment of water into the mixed layer. This balance is expressed by

$$(\overline{w'T'})_{h_o} = \left(\frac{dh_o}{dt} - w \right)(T_s - T_h) \tag{12}$$

where h_o = mixed-layer depth,

T_s = mixed-layer temperature,

T_h = temperature at the top of the thermocline, and

$\frac{dh_o}{dt}$ = the time variation of the mixed-layer due to wind mixing and convective overturning.

For entrainment to occur $(dh_o/dt) > 0$, that is, there can be no shallowing of the mixed layer unless w is upward. Integrating (10) over the mixed layer and substituting the boundary conditions gives

$$h_o \frac{dT_s}{dt} = \frac{Q_T}{\rho_w C_p} h_o - \left(\frac{dh_o}{dt} - w \right)(T_s - T_h) - \frac{Q_A}{\rho_w C_p}. \tag{13}$$

Expanding the total derivatives, neglecting solar radiation, and solving for $\partial h_o/\partial t$ gives

$$\frac{\partial h_o}{\partial t} = \frac{-h_o}{(T_s - T_h)} \left[\frac{\partial T_s}{\partial t} + \frac{\partial \bar{u} T_s}{\partial x} + \frac{\partial \bar{v} T_s}{\partial y} + \frac{\partial \bar{w} T_s}{\partial z} \right] - \frac{Q_A}{\rho_w C_p (T_s - T_h)} + w - u \frac{\partial h_o}{\partial x} - v \frac{\partial h_o}{\partial y} \tag{14}$$

which is a predictive equation for deepening shallowing of the mixed layer in terms of the local change in mixed-layer temperature.

To derive a similar predictive equation for the mixed-layer temperature Denman (1973) integrated (10) to an arbitrary depth z, and then over the mixed-layer depth yielding

$$\frac{h_o^2}{2} \frac{dT}{dt} = -\int_o^{h_o} (\overline{w'T'})_z \, dz - \frac{Q_A h_o}{\rho_w C_p} \tag{15}$$

where $-\int_o^{h_o} (\overline{w'T'})_z \, dz$ is the conversion of potential energy to kinetic energy by convection. If the turbulent kinetic energy is not varying in time, we may write

$$W + G - D = 0 \tag{16}$$

where G = kinetic energy input from the wind,

D = dissipation within the mixed layer, and

$W = -\int_o^{h_o} (\overline{w'T'})_z \, dz$

then substituting (16) into (15), expanding the total derivatives, and solving for $\partial T_s/\partial t$ yields

$$\frac{\partial T_s}{\partial t} = -\frac{2Q_A}{h_o \rho_w C_p} - \frac{2(G-D)}{h_o^2} - \frac{\partial \bar{u} T_s}{\partial x} - \frac{\partial \bar{v} T_s}{\partial y} - \frac{\partial \bar{w} T_s}{\partial z} \qquad (17)$$

which is the predictive equation for change in the mixed-layer temperature due to convection, entrainment mixing, or advection. Setting $Q_A = 0$, and/or $(G-D) = 0$, and/or $\bar{u}$, $\bar{v}$, and $\bar{w} = 0$ allows isolation of the cooling mechanisms for use individually and in combination. Substitution of (17) into (14) yields

$$\frac{\partial h_o}{\partial t} = \frac{Q_A}{\rho_w C_p (T_s - T_h)} + \frac{2(G-D)}{h_o (T_s - T_h)} - u\frac{\partial h_o}{\partial x} - v\frac{\partial h_o}{\partial y} + w \qquad (18)$$

which is the predictive equation for changes in the mixed-layer depth as used in the present model.

A partitioning procedure was used to divide the total available stress, τ_a, from the boundary layer into one fraction for the production of turbulence, τ_o, and the remainder $(\tau_a - \tau_o)$, for the generation of wind-driven currents.

$$\tau_o = \tau_a \, \mathrm{EXP} \left(- \frac{h_o}{C z_o} \right) \qquad (19)$$

where τ_a = total stress available from boundary-layer model,

h_o = mixed-layer depth,

z_o = roughness length, and

C = a constant (10^4) (after Fraim 1973).

Kraus and Turner (1967) assuming a value for τ_o, specified the mechanical energy input (G) in equations (16), (17), and (18) as

$$G = \frac{1}{g\alpha\rho_a} \left(\frac{\rho_a}{\rho_w} \right)^{3/2} u_* \tau_o \qquad (20)$$

where g = gravitational acceleration,

$\alpha = (1/\rho_w)(d\rho_w/dt)$, coefficient of expansion

ρ_a = air density,

ρ_w = sea water density,

u_* = atmospheric friction velocity, = $\sqrt{\tau_a/\rho_a}$, and

τ_o = that part of atmospheric surface stress used to produce turbulent mixing.

The dissipation (D) was set equal to zero.

The calculation for the ocean velocities was by means of Ekman-spiral theory. The theory specifies a depth (Z_e) at which the current direction has reversed from its surface direction, the current is EXP(-π) of its surface value, and below which the wind has no direct influence. The velocity components of the ocean within the spiral layer are

$$u = \frac{(\tau_a - \tau_o)\cos\alpha}{\rho_w (2f\frac{\mu}{\rho_w})^{\frac{1}{2}}} \text{EXP}(-BZ)[\cos(-BZ) - \sin(-BZ)] \quad (21)$$

$$v = \frac{(\tau_a - \tau_o)\sin\alpha}{\rho_w (2f\frac{\mu}{\rho_w})^{\frac{1}{2}}} \text{EXP}(-BZ)[\cos(-BZ) - \sin(-BZ)] \quad (22)$$

where $Z_e = \pi/B$, specifies the Ekman depth,

$B = [f/2\mu/\rho_w]^{\frac{1}{2}}$,

f = coriolis parameter,

ρ_w = sea water density,

μ = vertical eddy coefficient of viscosity,

z = depth, and

α = atmospheric inflow angle.

Integration of (21) and (22) over the Ekman depth (Z_e) gives the net mass transport in the Ekman layer

$$M_x = (\tau_a - \tau_o)\cos\alpha/f \tag{23}$$

$$M_y = (\tau_a - \tau_o)\sin\alpha/f. \tag{24}$$

From these mass transport equations it is possible to calculate the mean ocean velocities in the mixed layer

$$\bar{u}Z_e = M_x/\rho_w \tag{25}$$

$$\bar{v}Z_e = M_y/\rho_w. \tag{26}$$

The horizontal velocities in the layer are related to the vertical velocity w by the continuity equation

$$\frac{\partial w}{\partial z} = -\left(\frac{\partial u}{\partial x} + \frac{\partial v}{\partial y}\right). \tag{27}$$

Equations (17) and (18) give two equations for three unknowns (T_s,h_o,T_h). A return flow is calculated for the layer between 130 meters and the new mixed-layer depth. It is assumed to have the same mass transport as the opposing current in the mixed layer, and to be centered on a point 2/3 of the distance from 130 meters to h_o. The below-layer gradient is adjusted by the return flow, upwelling, and downwelling. The new T_h is the temperature at the intersection of the new below-layer gradient and the new mixed-layer depth. This relation is given by

$$T_h = T_B + \left(\frac{\partial T}{\partial z}\right)(Z_B - h_o)$$

where $\partial T/\partial z$ = is the below-layer gradient,

T_B = temperature at top of the undisturbed layer = 20 C, and

Z_B = depth of top of undistirbued layer = 130 m.

III. DISCUSSION OF RESULTS

It was the intent of this study to use a sea-air interacting numerical model to simulate the effects upon the ocean of a hurricane moving across it. The reasons for conducting the study were: 1) to investigate the cause of low sea-surface temperatures in the wake of a hurricane, and 2) to determine the effects on the ocean for different speeds of storm movement.

Changes to the mixed-layer depth are controlled by Equations (17) and (18). Convective mixing is represented by the first term in both equations. Entrainment mixing involves the second term in both equations. Advection is described by the remaining terms in the equations. According to the two equations entrainment mixing and convection can only cool and deepen the mixed layer. It has been assumed that Q_A is positive by assuming a wind-dominated regime. On the other hand, since ocean velocity values can be both negative and positive, the advection terms can both warm and cool, shallow and deepen the mixed layer.

This discussion is divided into three parts: 1) a comparison with the results of Fraim (1973), 2) a discussion of the relative importance in this model of the mechanisms discussed above, and 3) a discussion of the effect of the hurricane translational speed on changes in the ocean.

A. COMPARISON WITH FRAIM'S RESULTS

Before attempting to move the hurricane, it was necessary to establish that the stationary version of the present model yielded reasonable results. For the initial experiment, the 200 x 3 grid (Figure 1) was defined with a 3 km grid spacing as was the 100 x 1 grid in Fraim's model. Profiles of values at 12 hours for the present model are shown in Figure 2. A comparison of maximum and minimum values for Fraim's model and the present model are listed in Table I.

The first point of comparison between the two studies is the hurricane portion of the model. The initial conditions for both hurricanes were the same: air temperature T_a = 29C, radius of maximum wind r_i = 27km, and maximum tangential wind V_{θ_i} = 30m/sec. There were some differences. Fraim did not constrain the maximum tangential wind or the radius of maximum wind. In the present model, for this experiment, the maximum tangential wind was forced to increase sinsuoidally from 30m/sec to 50m/sec at 12 hours. Also, a limit of $r_i \leq 60$ km was set on the radius of maximum wind.

The tangential wind profile (bottom, Figure 2) is characterized by a rapid increase with radius to its maximum value at r_o = 60 km (Equation (2)), a slow decline to its value at r_o (Equation (1)), and a more rapid decline to the outer boundary value. From r_o to $2r_o$ the wind is allowed to drop off to 5m/sec. At r_o the change in the wind profile is abrupt and therefore easily detected. The radius r_o tends to be the limit of applicability of the assumption of axisymmetry at upper levels, although the assumption is good to

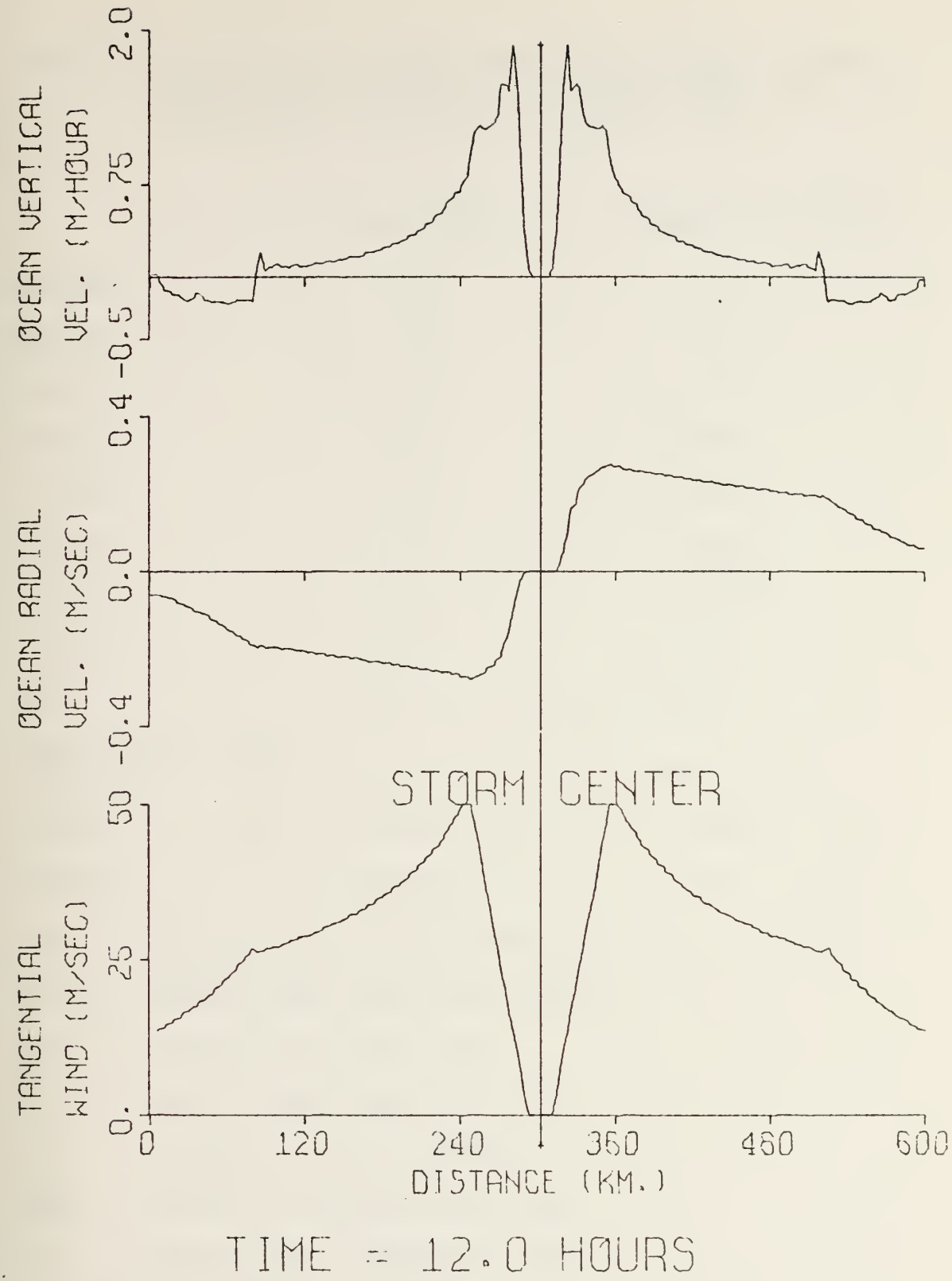

Figure 2. 12-Hour Predicted Values of Tangential Wind, Ocean Radial Velocity, and Ocean Vertical Velocity for the Stationary Diametrical Hurricane Model on a 3 km Grid.

Table I. Comparison Between Some 12-Hour Values of the Fraim Radial Stationary Hurricane Model and the Diametrical Stationary Hurricane Model.

	Fraim Model	Diametrical Model
Max ORV	.48	.28
Max DW	.03	.21
Max UW	3.35	1.88
Min MLD	4.31	21.23
Max MLD	51.23	58.20
Min MLT	25.26	28.84
Max MLT	30.43	30.00
Max TW	55.58	50
RMW	42	60
Area average ocean heat loss	930	371
Min TT	19.80	26.90
Max TT	29.99	30

ORV - ocean radial velocity (m/sec)

DW, UW - downwelling, upwelling (m/hr)

MLD - mixed-layer depth (m)

MLT - mixed-layer temperature (C)

TW - tangential wind (m/sec)

RMW - radius of maximum wind (km)

TT - thermocline temperature (C)

Heat loss (cal/cm^2)

a greater radius at lower levels. Because r_o expands with intensification (r_o = 225 km at 12 hours vs. 150 km at 0 hours), the wind velocity value at the outer boundary of the hurricane model has increased from 5m/sec to 12.5m/sec. The maximum tangential wind (Table I) was about 10% greater in Fraim's model than that of the present model due to lack of constraint on the maximum wind value.

The ocean radial velocity (actually the x-component of the horizontal velocity)(middle, Figure 2) responds directly to the stress imparted by the tangential wind (Equations (21) and (22)). Ocean velocity values are calculated by integrating the x-component of the Ekman current over the mixed-layer depth. Fraim integrated the mass transport over a shallower depth thus giving a larger velocity (Fraim's results, Table I).

As the ocean radial velocity directly follows the tangential wind, the ocean vertical velocity (top, Figure 2) follows the gradient of the radial velocity. The result is that the maximum upwelling occurs at the point of maximum increase of ocean radial velocity, i.e., between the center of the storm and the radius of maximum wind. Maximum downwelling occurs at r_o where the ocean radial velocity drops sharply. Fraim's model upwelling (Table I) is stronger because the radius of maximum wind was smaller. The Fraim model had no major downwelling because tangential wind profile was not altered in the r_o to $2r_o$ region.

The radius of the maximum mixed layer depth, minimum mixed-layer temperature, and minimum thermocline temperature,

(Figure 3) is the same, and coincides with the radius of maximum wind. Coinciding with the radius of maximum upwelling are the minimum mixed layer depth, and pips of warming in the mixed-layer (T_s) and thermocline (T_h) temperatures. The pips appear to be due to a lack of cooling due to upwelling. The minimum mixed-layer temperature (Table I) is much smaller in Fraim's model because it did not have the thermocline layer return flow discussed in Chapter II B. 1. Lack of a return flow of water allowed strong cooling of the thermocline layer in the Fraim model which created a large T_s-T_h difference (Table I) and retarded deepening of the mixed layer. Consequently, the area-averaged heat loss in Fraim's model was more than twice the loss in the present model (see Table I). Most of the heat loss is concentrated within 100 km of the center. Advection of water both horizontally and vertically acts to cool or warm the thermocline layer. Warming in the upper portion of this layer increases the below-layer gradient while cooling decreases the gradient. A change in the below-layer gradient is thus associated with the temperature at the top of the thermocline, that is, the thermocline temperature, since the temperature at the level of no-motion is held constant. Stronger upwelling in Fraim's model (Table I) accounts for the shallower mixed-layer depth minimum and seems to indicate a higher maximum mixed-layer temperature. The comparison between the models shows the results are similar, however, due to the differences mentioned above the present model yielded more reasonable results.

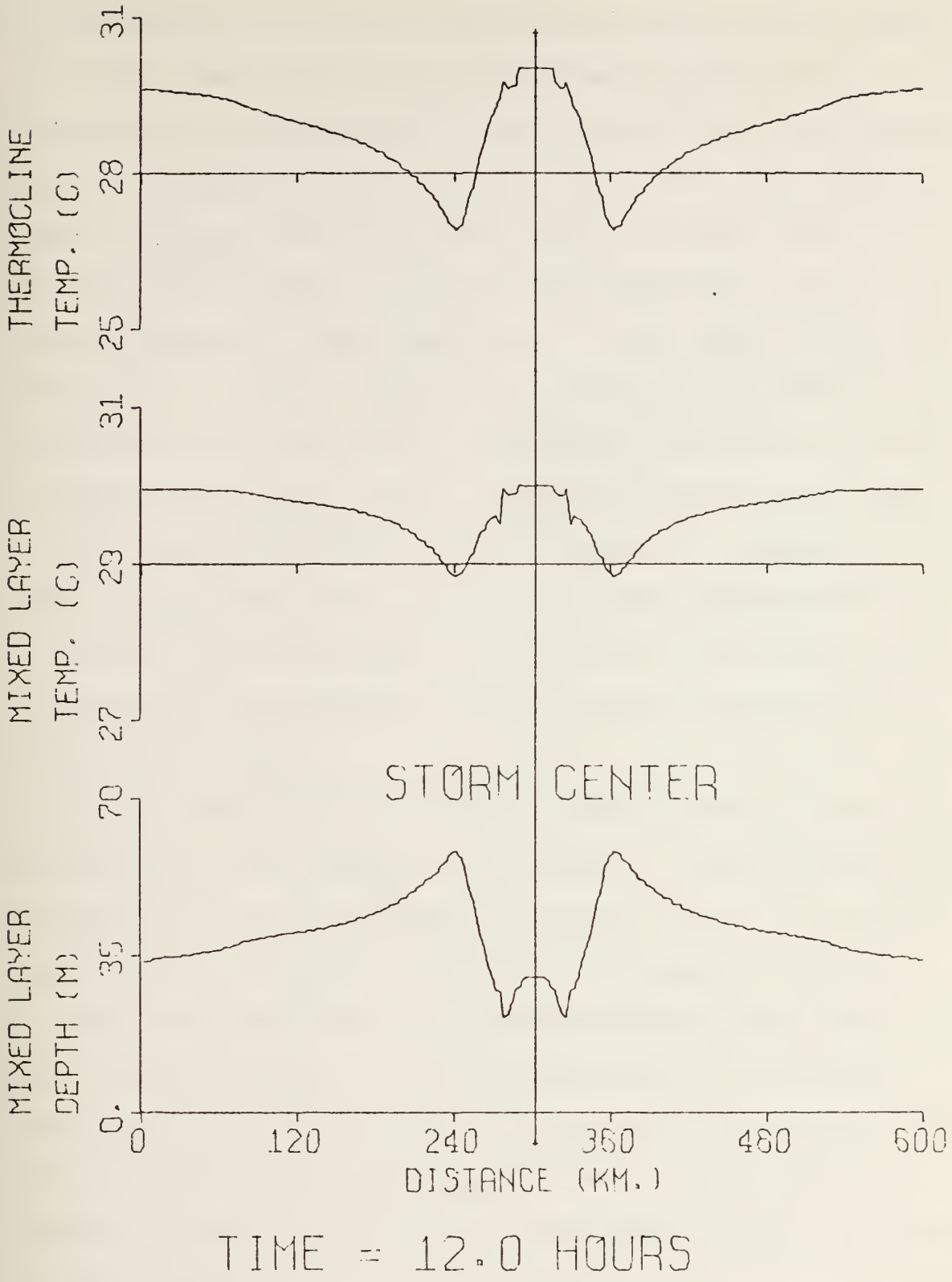

Figure 3. 12-Hour Predicted Values of Mixed-Layer Depth, Mixed-Layer Temperature, and Thermocline Temperature for the Stationary Diametrical Hurricane Model on a 3 km Grid.

B. DISCUSSION OF COOLING MECHANISMS BENEATH A MOVING STORM

As the comparison of the present model with Fraim's was considered satisfactory, it was decided that the results warranted progressing to a moving storm. The storm was allowed to interact with the ocean until a maximum wind of 50 m/sec was achieved so as to allow examination of the ocean's response to the same storm. A new limit of $r_i \leq 45$ km was placed on the radius of maximum wind. The 200 x 3 grid spacing was expanded to 6 km giving a 12 km by 1200 km rectangle in the open ocean. Starting point for the center of the storm was the 900 km point (Figure 8). Movement of the storm was from right to left at 1 grid increment per 2, 3, 5, and 7 time increments, or 6 km per 16, 24, 40, and 56 minutes which corresponds to 11.84, 7.89, 4.75, and 3.39 knots respectively.

A time cross-section of the 4.75 knot storm was drawn for the mixed-layer temperature response (Figure 4, Table II) and mixed-layer depth response (Figure 5, Table III) of the ocean to the mechanisms indicated in the figures. The 750 km point was chosen for this section because during the 30 hour forecast period it experienced passage of the most interesting parts of the storm i.e. the radii of maximum wind, the radii of maximum upwelling, and the no-stress zone of the eye. Figure 8 can be used to see the relative locations of these zones.

As shown in Figure 4, advection alone has virtually no impact on the mixed-layer temperature, though in the absence of deepening (Figure 5) shows a slight warming as mentioned

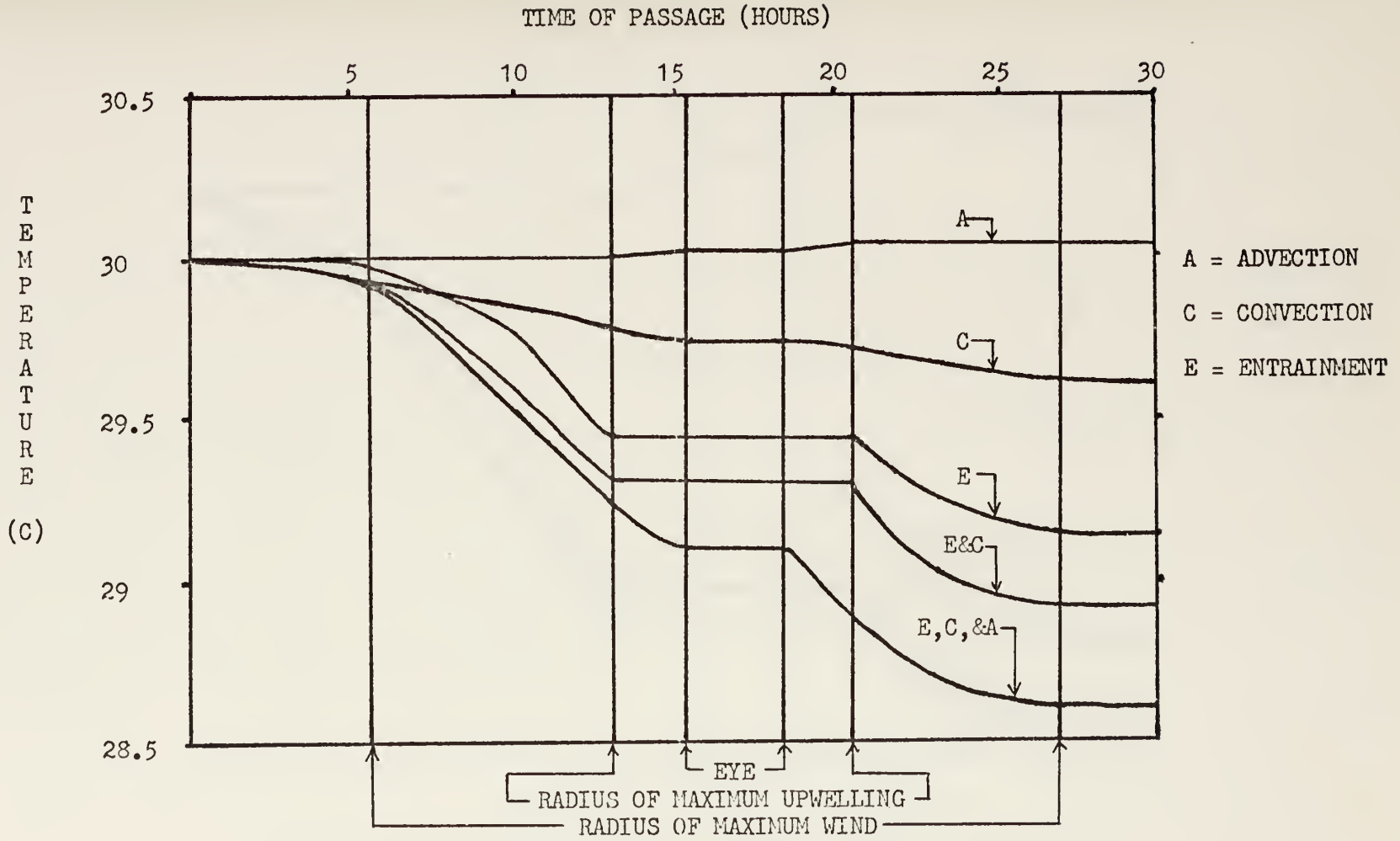

Figure 4. Time Cross-Section of Mixed-Layer Temperature at the 750 km Point for the 4.75 Knot Storm.

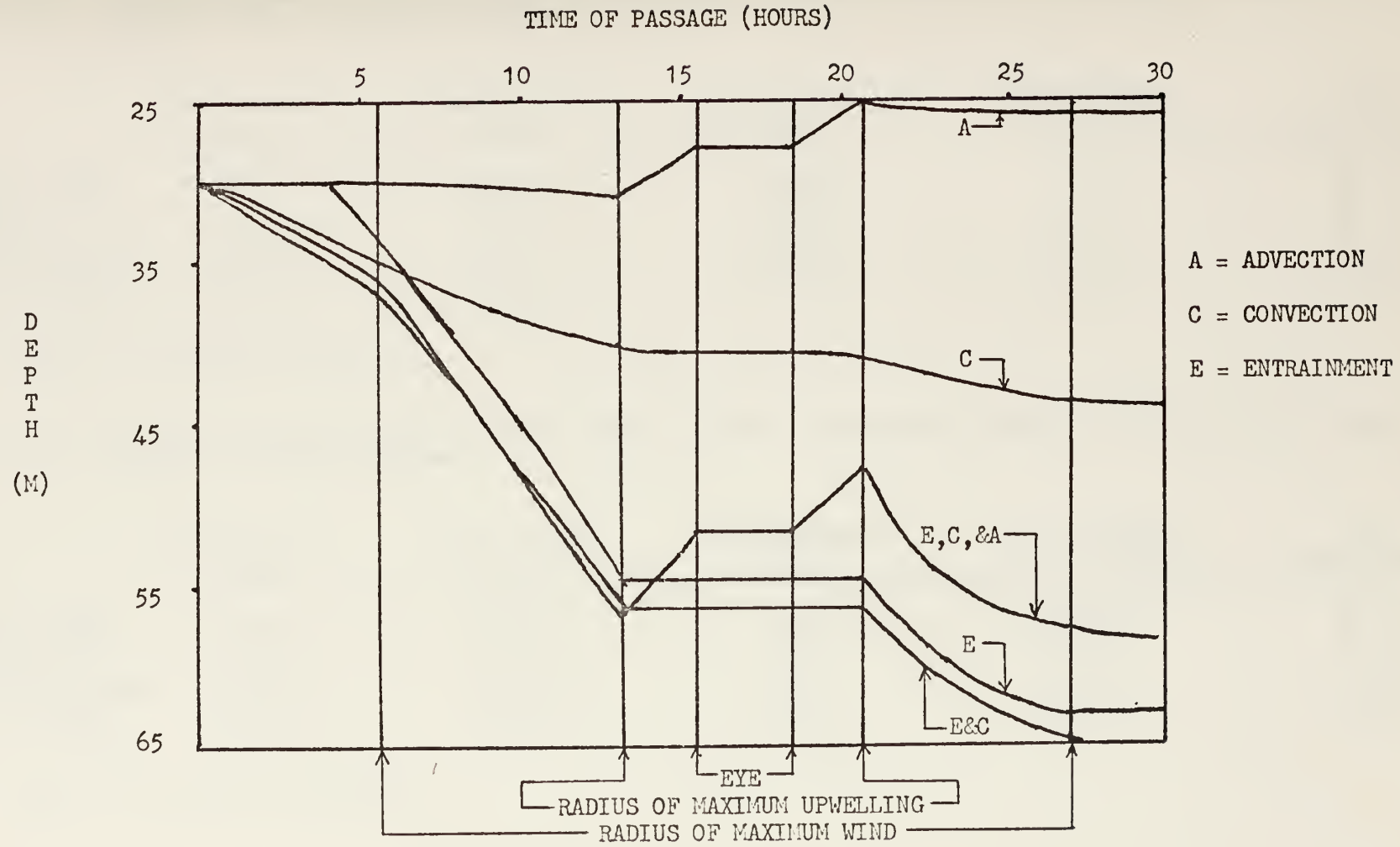

Figure 5. Time Cross-Section of Mixed-Layer Depth at the 750 km Point for the 4.75 Knot Storm.

Table II. Actual Values of Mixed-Layer Temperature for Key Points of Passage at the 750 km Point of the 4.75 Knot Storm.

	Advection Only	Convection Only	Entrainment Only	Entrainment & Convection	All Mechanisms
leading RMW	30	29.93	29.98	29.91	29.92
leading UW	30	29.77	29.45	29.32	29.25
no stress zone	30.02	29.74	29.45	29.32	29.10
trailing UW	30.04	29.72	29.45	29.32	28.91
trailing RMW	30.04	29.61	29.14	28.94	28.61

*see Table I for abbreviations

Table III. Actual values of Mixed-Layer Depth for Key Points of Passage at the 750 km Point of the 4.75 Knot Storm.

	Advection Only	Convection Only	Entrainment Only	Entrainment & Convection	All Mechanisms
leading RMW	29.96	34.73	33.28	36.55	35.64
leading UW	30.85	39.98	54.6	56.4	56.67
no stress zone	27.94	40.43	54.6	56.4	51.16
trailing UW	25.29	40.92	54.6	56.4	47.66
trailing RMW	25.79	43.70	62.79	65	60

*see Table I for abbreviations

in Chap. III. A. Entrainment mixing and convection appear to dominate outside the radii of maximum upwelling with the maximum effect being inside the radii of maximum wind. Of the two, entrainment mixing is the stronger cooling mechanism. It is interesting to note that convection alone contributes to the small amount of cooling within the radii of maximum upwelling. All mechanisms combined appear to contribute to cooling between the radii of maximum upwelling, although no changes occur during passage of the eye. It appears that horizontal ocean velocities have little direct effect on the mixed layer, but that vertical velocities have a significant effect.

As shown in Figure 5, advection alone has a small effect in changing the mixed layer. Again, entrainment mixing and convection appear to dominate outside the radii of maximum upwelling with the maximum effect being inside the radii of maximum wind. Of the two, entrainment is definitely dominant in deepening the mixed layer, although inside the radii of maximum upwelling convection is the only mechanism that deepens the mixed layer. Inside the radii of maximum upwelling, advection alone is responsible for shallowing the mixed layer. In conjunction with entrainment mixing and convection, the effect of advection increases.

One cannot completely separate the mechanisms since there is a complex interaction between them in the ocean. However, Leipper (1967) interpreted baththermograph data before and after passage of the hurricane Hilda in the Gulf of Mexico during 1964 as follows: 1) cold water was upwelled due to

divergence in the region near the center of the storm, and 2) warm water farthest from the storm path gave evidence of having been mixed by surface cooling or by mechanical mixing or both. As shown in Figure 9, the lowest mixed-layer temperatures are in the vicinity of the storm center. The warmer water toward the boundary of the storm (Figure 8) shows evidence of mixing (implied by mixed layer deepening).

A set of profiles of temperature change from the initial temperatures in the ocean due to hurricane passage is shown in Figure 6. The profiles show cooling down to 30 m (except the profile for advection only) then warming down to the mixed-layer depth. Entrainment of colder thermocline water cools the mixed layer and warms the thermocline layer to form a new mixed layer. At the mixed-layer depth in the model there is a discontinuity denoted earlier by $T_s - T_h$. Below the mixed layer only those mechanisms involving advection show distinct cooling. Return flow in the thermocline layer and upwelling are responsible for the cooling. The 750 km point is 120 km behind the storm center at 30 hours. As a result Figure 6 agrees with Federov's (1973) Type A thermal structure change profile of two layers of cooling separated by a layer of warming.

The effect of the return flow in the thermocline layer can also be seen in Figure 7. Entrainment mixing and convection singly and together have an insignificant effect on the below-layer gradient. The rapid decrease of the below-layer gradient for advection alone shows that for intense upwelling there is strong cooling in the upper part of the

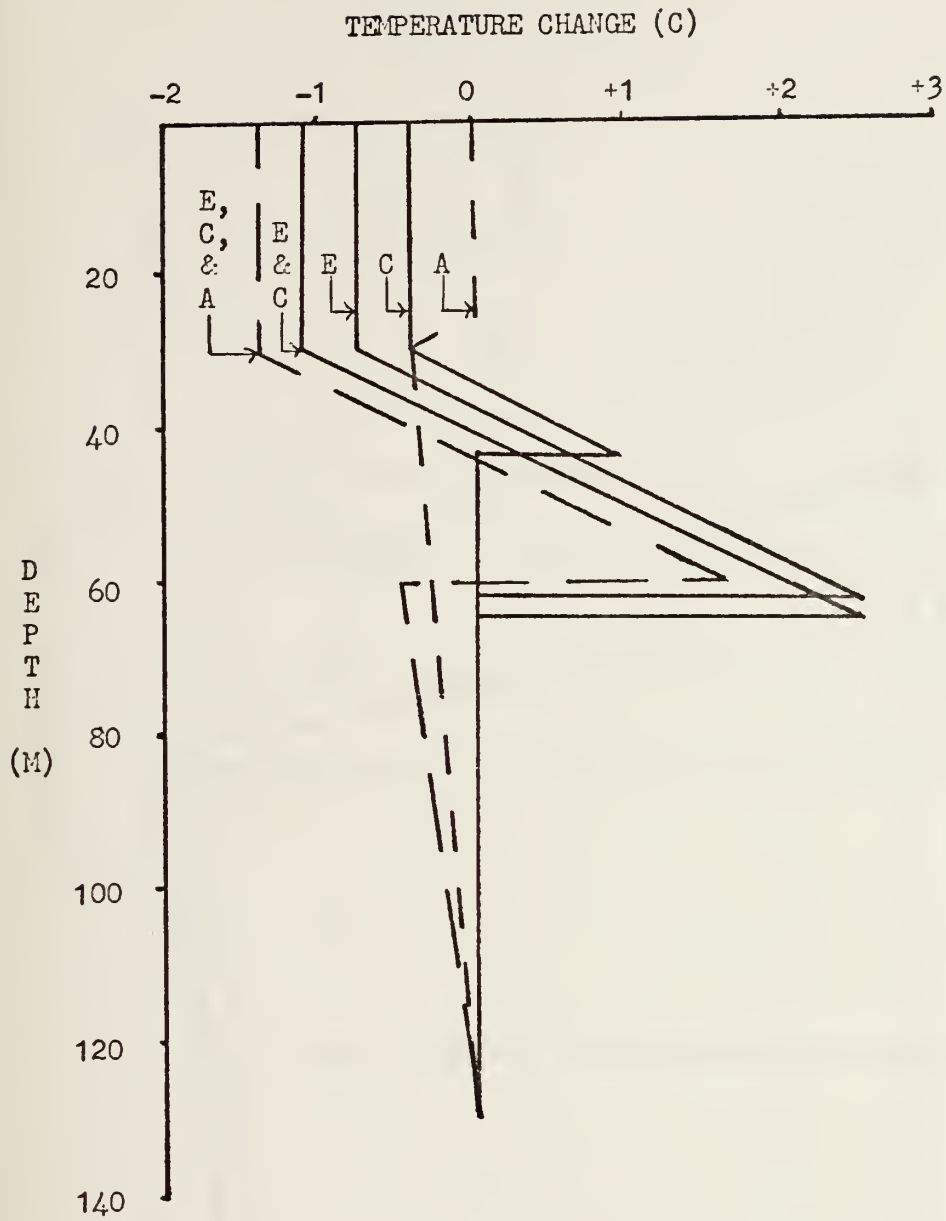

Figure 6. Change in Thermal Structure at the 750 km Point After Passage of the 4.75 Knot Storm. (The initial conditions were MLD = 30 m, MLT = 30 C with a linear temperature decrease to a value of 20 C at 130 m.)

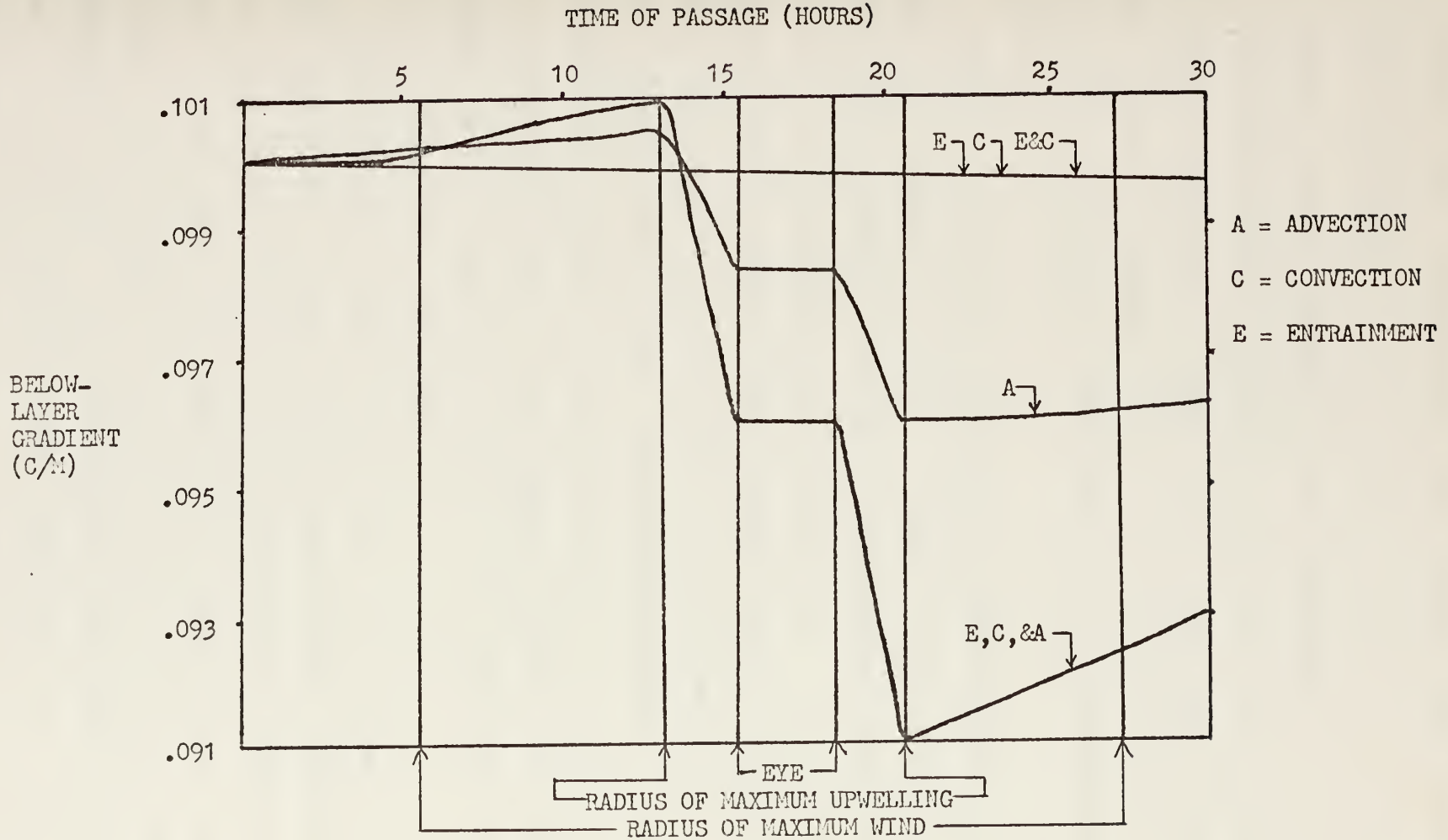

Figure 7. Time Cross-Section of Below-Layer Gradient at the 750 km Point for the 4.75 Knot Storm.

thermocline layer indicating a more intense upwelling than for advection alone.

C. EFFECT OF STORM MOVEMENT ON OCEAN RESPONSE

The second purpose listed for the study was to determine the effect of movement of the storm on the ocean's response to the storm. In Table IV is listed some maximum and minimum values of key parameters for several storm translational speeds.

Changes in the mixed layer due to storm movement are comparatively easy to explain. Slower-moving storms have more time at a given location for entrainment mixing and convection to cool and deepen the mixed layer. For the stationary storm the downwelling maximum nearest the storm center (see Figure 10) has added to the deepening but perhaps retarded the cooling. The anomalous spikes of downwelling (for instance at the 900 km point in Figure 10) are due to the sharp drop in the tangential wind at the storm boundary and the mixed-layer depth spikes generated due to the stationarity of the storm.

Increasing heat flux to the storm with increasing storm speed (Table IV) is due to fast moving storms extracting more heat because of continuously encountering uncooled 30 C water. Radial heat flux (Table IV) is due to heat flow in currents out through the mixed layer and in through the thermocline layer. For a stationary storm advection supplies more heat than it removes. This seems to be the source of warm water for the mixed-layer temperature pips (Figure 11).

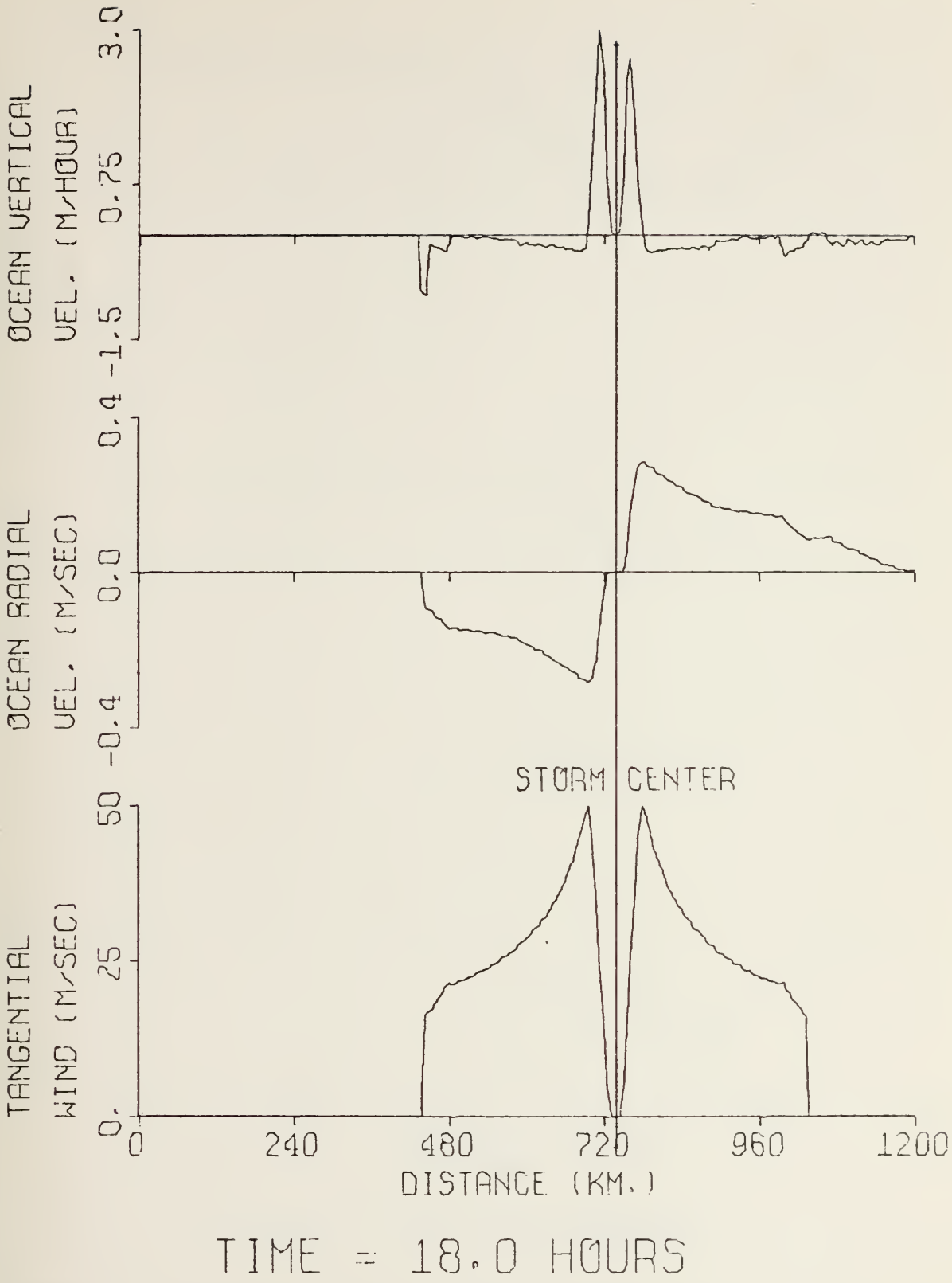

Figure 8. 18-Hour Predicted Values of Tangential Wind, Ocean Radial Velocity, and Ocean Vertical Velocity for a Hurricane Moving at 4.75 Knots.

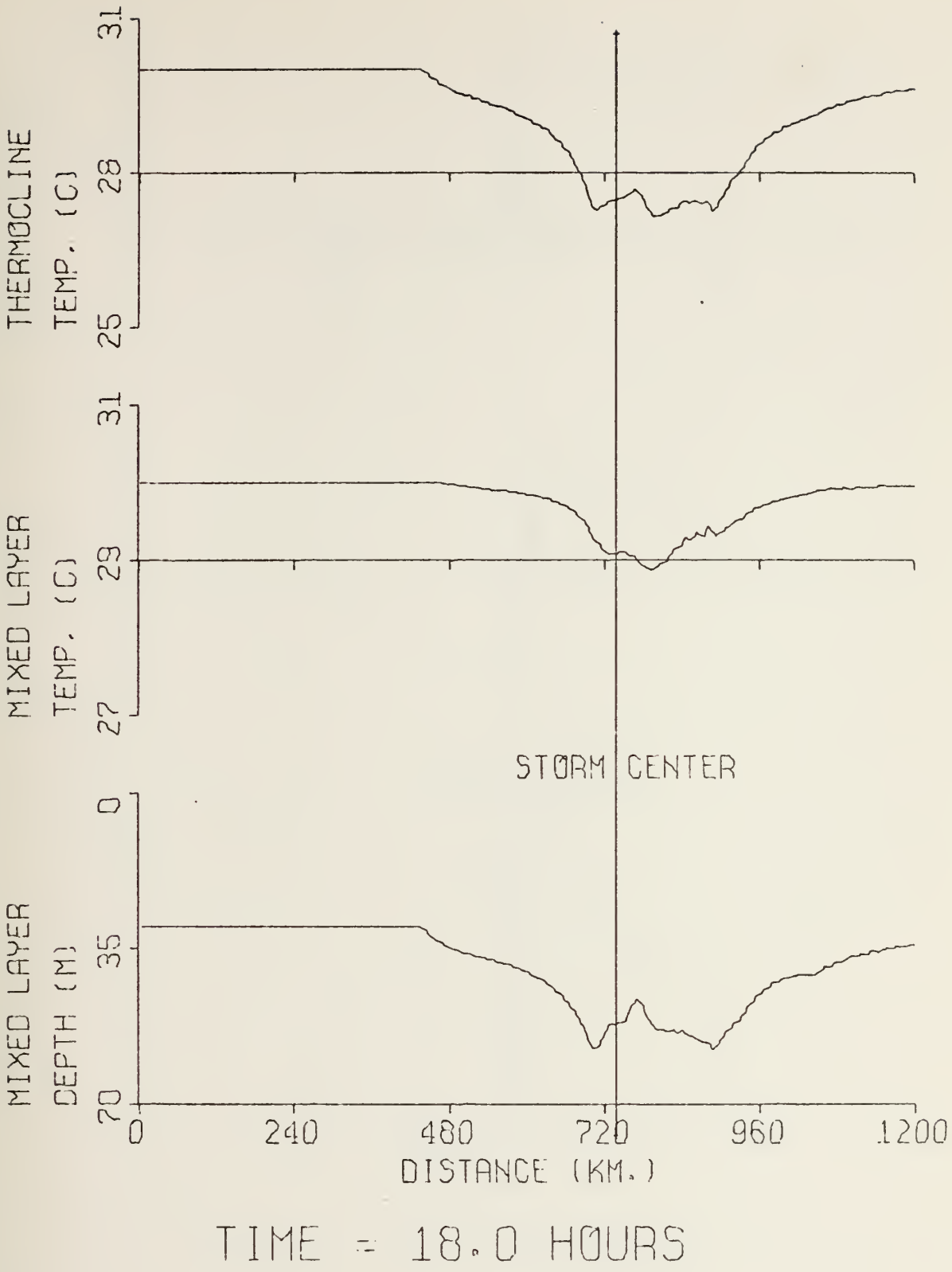

Figure 9. 18-Hour Predicted Values of Mixed-Layer Depth, Mixed-Layer Temperature, and Thermocline Temperature for a Hurricane Moving at 4.75 Knots.

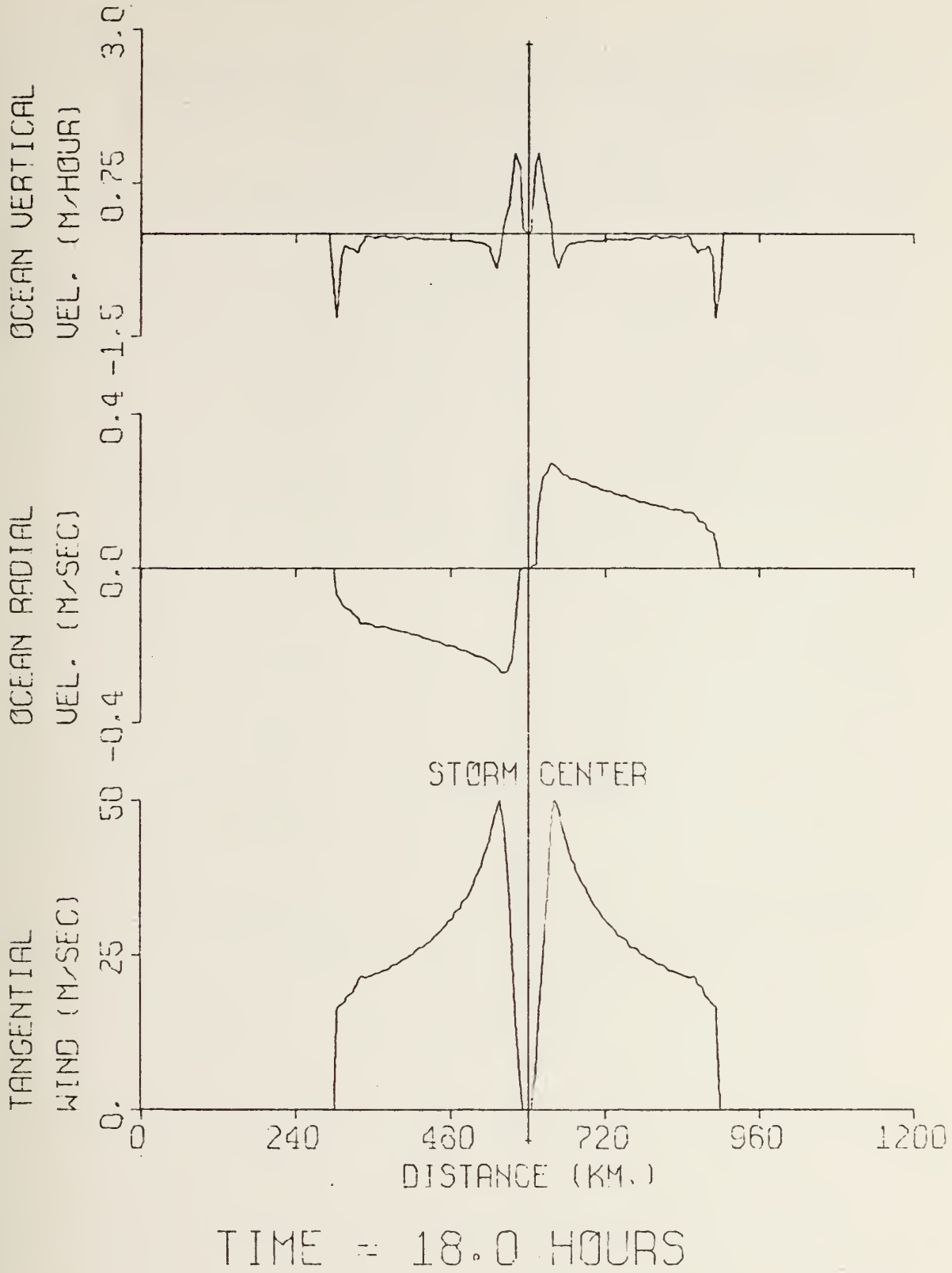

Figure 10. Same as Figure 8 Except for a Stationary Hurricane.

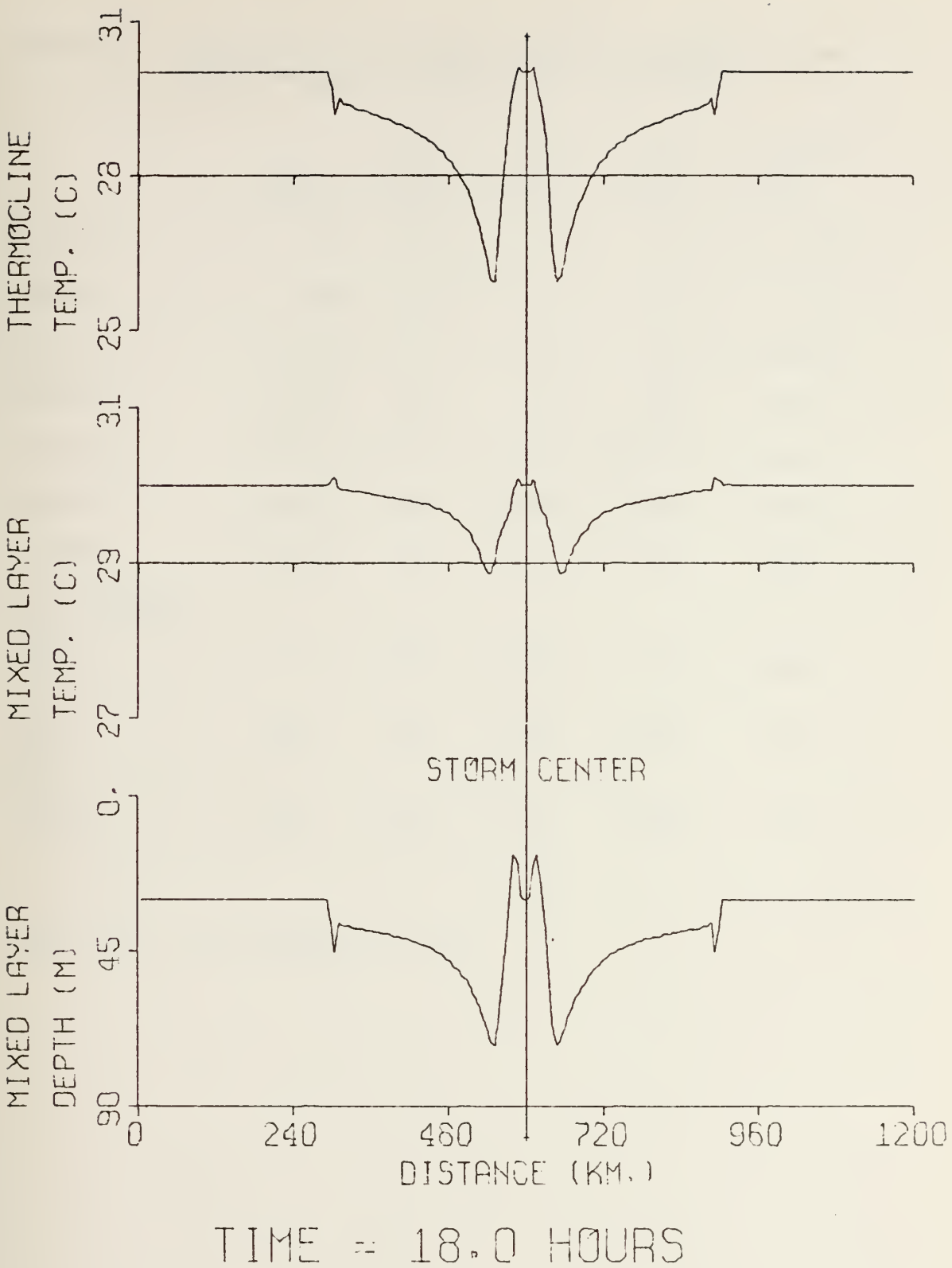

Figure 11. Same as Figure 9 Except for a Stationary Hurricane.

Table IV. Comparison of Parameters for Several Storm Translational Speeds at t = 18 Hours.

	Stat	3.39 kts.	4.75 kts.	7.89 kts.	11.84 kts.
max ORV	.27	.28	.29	.29	.29
max DW	.48	.32	.28	.27	.21
max UW	1.18	3.10	2.98	2.78	2.60
min MLD	17.18	30	30	30	30
max MLD	72.60	61.62	57.91	54.78	53.94
min MLT	28.85	28.86	28.88	29.06	29.25
max MLT	30.09	30	30	30	30
area average ocean heat loss	- 29	265	325	352	335
radial heat flux	-146	58	89	103	92
heat lost to storm	156	161	163	168	174

*see Table I for abbreviations

The apparent reversal of radial heat flux values for the two fastest storms in unexplained.

A sustained upwelling for 18 hours duration would account for the shallow minimum mixed-layer depth (Table IV). By the equation for continuity (Equation (27)) the integrated vertical velocity is equal to the horizontal velocity divergence times the integrated depth. Therefore the maximum upwelling value for the stationary storm is small because of the mixed-layer depth in which it occurs (Figures 10 and 11). For a moving storm the leading upwelling zone the upwelling is more intense because it occurs in the deepest mixed layer (Figures 8 and 9). Maximum downwelling intensities are governed by mixed-layer depth also (Figures 8, 9, 10 and 11). Maximum values for the ocean radial velocity are much the same because the mean mixed-layer depths at the radius of maximum ocean radial velocity are nearly the same. The ocean radial velocity profiles are altered slightly due to mixed-layer depth considerations (Figures 8 and 10).

IV. SUMMARY AND CONCLUSION

It was the intent of this study to use a numerical model to simulate the effects of a hurricane moving across the ocean. In such numerical models the inherent limitations include the finite differencing scheme as well as the initial and boundary conditions. Imposed limitations involve assumptions associated with applying the model.

For this study a simple model was used for both the hurricane and the ocean. A bound was set on the hurricane maximum wind in order to standardize the storm input to the ocean. There were several key assumptions about the way in which the ocean and storm interact: 1) wind stress was partitioned into making currents and turbulence based on the mixed-layer depth, 2) ocean currents were assumed to be in Ekman balance and to respond immediately to changes in the stress pattern, 3) it was assumed that there were no gradients of temperature or ocean velocity across the path of the storm, 4) the storm was assumed to be wind-dominated, and 5) since the storm was mature at initiation the total stress imparted exponentially until 95% of the total stress was imparted to the ocean at 9 hours.

In answer to the two main questions of interest: 1) cooling of the ocean appears to be primarily due to entrainment and convection except in intense upwelling within the region of maximum wind. In this region all mechanisms contribute to cooling of the mixed layer, 2) slow moving storms

cool and deepen the mixed layer more than do fast moving storms. Waves in the mixed-layer depth due to internal waves on the mixed-layer thermocline layer interface postulated by Geisler (1970) were not seen. This is due to the thermodynamic nature of the model under study here compared to the hydrodynamic nature of Geisler's model.

In summary, the results are satisfactory within the limits of the model. The logical course to follow is to reduce the number of assumptions used. In a model with as many simultaneous interactions as this one, the task is one to be taken slowly, in small increments.

BIBLIOGRAPHY

1. Cardone, V. J., 1969: Specification of the Wind Distribution in the Marine Boundary Layer for Wave Forecasting, New York University, School of Engineering and Sciences, Scientific Report GSL-TR69-1, University Heights, New York.

2. Denman, K. L., 1973: A Time-Dependent Model of the Upper Ocean, Journal of Physical Oceanography, 3 173-184.

3. Elsberry, R. L., Pearson, N. A. S., and Corgnati, L. B., 1974: A Quasi-Empirical Model of the Hurricane Boundary Layer, Journal of Geophysical Research, 79, 3033-3040.

4. Fedorov, K. N., 1973: The Effect of Hurricane and Typhoons on the Upper Active Ocean Layers, Oceanology, 12, 329-332.

5. Fischer, E. L., 1958: Hurricanes and the Sea-Surface Temperature Field, J. Meteor., 15, 328-333.

6. Fraim, T. S., 1973: Oceanic Thermal Response to a Time-Dependent Hurricane Model, MS Thesis, Naval Postgraduate School, Monterey, California.

7. Geisler, J. E., 1970: Linear Theory of the Response of a Two Layer Ocean to a Moving Hurricane, Geophysical Fluid Dynamics, 1, 249-272.

8. Gray, W. M. and Shea, D. J., 1973: The Hurricanes' Inner Core Region, 2, Thermal Stability and Dynamic Characteristics, J. Atmos. Sci., 30, 1565-1576.

9. Jordan, C. L., 1964: On the Influence of Tropical Cyclones on the Sea-Surface Temperature Field, Proc. Symp. Trop. Meteor., New Zealand Meteor. Service, Wellington, 614-622.

10. Kraus, E. B., and Turner, J. S., 1967: A One-Dimensional Model of the Seasonal Thermocline, Tellus, 19, 88-106.

11. Leipper, D. F., 1967: Observed Ocean Conditions and Hurricane Hilda, 1964, J. Atmos. Sci., 24, 182-196.

12. O'Brien, J. J., 1967: The Non-Linear Response of a Two-Layer, Baroclinic Ocean to a Stationary, Axially-Symmetric Hurricane: Part II, J. Atmos. Sci., 24, 208-215.

13. O'Brien, J. J., 1968: The Response of the Ocean to a Slowly Moving Cyclone: NCAR Manuscript, No. 68-57, pp. 36.

14. O'Brien, J. J. and Reid, R. O., 1967: The Non-Linear Response of a Two-Layer, Baroclinic Ocean to a Stationary, Axially-Symmetric Hurricane: Part I, J. Atmos. Sci., 24, 197-207.

15. Riehl, H., 1963: Some Relations Between Wind and Thermal Structure of Steady-State Hurricanes, J. Atmos. Sci., 20, 276-287.

INITIAL DISTRIBUTION LIST

		No. Copies
1.	Defense Documentation Center Cameron Station Alexandria, Virginia 22314	2
2.	Library, Code 0212 Naval Postgraduate School Monterey, California 93940	2
3.	Professor R. L. Elsberry, Code 51Es Department of Meteorology Naval Postgraduate School Monterey, California 93940	7
4.	Professor D. F. Leipper, Code 58Lr Department of Oceanography Naval Postgraduate School Monterey, California 93940	1
5.	CAPT R. N. Trapnell, Jr., USAF Det 1, 1st WWg COMNAVMAR Box 17 FPO San Francisco 96630	3
6.	Air Weather Service (AWVAS/TF) Scott AFB, Illinois 62225	1
7.	Professor R. L. Haney, Code 51Hy Department of Meteorology Naval Postgraduate School Monterey, California 93940	1
8.	Department of Oceanography, Code 58 Naval Postgraduate School Monterey, California 93940	3
9.	Oceanographer of the Navy Hoffman Building No. 2 200 Stovall Street Alexandria, Virginia 22332	1
10.	Office of Naval Research Code 480 Arlington, Virginia 22217	1
11.	Library, Code 3330 Naval Oceanographic Office Washington, D. C. 20373	1

12. Dr. Robert E. Stevenson — 1
Scientific Liaison Office, ONR
Scripps Institution of Oceanography
La Jolla, California 92037

13. SIO Library — 1
University of California, San Diego
P. O. Box 2367
La Jolla, California 92307

14. Department of Oceanography Library — 1
University of Washington
Seattle, Washington 98105

15. Department of Oceanography Library — 1
Oregon State University
Corvallis, Oregon 97331

16. Commanding Officer — 1
Fleet Numerical Weather Central
Monterey, California 93940

17. Commanding Officer — 1
Environmental Prediction Research Facility
Monterey, California 93940

18. Department of the Navy — 1
Commander Oceanographic System Pacific
Box 1390
FPO San Francisco 96610